A Mutation in *SNAP29,* Coding for a SNARE Protein Involved in Intracellular Trafficking, Causes a Novel Neurocutaneous Syndrome Characterized by Cerebral Dysgenesis, Neuropathy, Ichthyosis, and Palmoplantar Keratoderma

Eli Sprecher,[1,4] Akemi Ishida-Yamamoto,[7] Mordechai Mizrahi-Koren,[1,5] Debora Rapaport,[8] Dorit Goldsher,[2,4] Margarita Indelman,[1] Orit Topaz,[1,4] Ilana Chefetz,[1,4] Hanni Keren,[1] Timothy J. O'Brien,[9] Dani Bercovich,[10] Stavit Shalev,[11] Dan Geiger,[6] Reuven Bergman,[1,4] Mia Horowitz,[8] and Hanna Mandel[3,4]

[1]Department of Dermatology and Laboratory of Molecular Dermatology, [2]MRI Institute, [3]Metabolic Disease Unit and Department of Pediatrics B, Rambam Medical Center; [4]Rappaport Faculty of Medicine, [5]Biotechnology Interdisciplinary Unit, and [6]Computer Science Department, Technion-Israel Institute of Technology, Haifa, Israel; [7]Department of Dermatology, Asahikawa Medical College, Asahikawa, Japan; [8]Department of Cell Research and Immunology, Tel Aviv University, Ramat Aviv, Israel; [9]Department of Obstetrics and Gynecology, University of Arkansas for Medical Sciences, Little Rock; [10]Human Molecular Genetics & Pharmacogenetics, Migal-Galilee Technology Center, Kiryat-Shmona, Israel; [11]Genetic Institute, Ha'emek Medical Center, Afula, Israel

Neurocutaneous syndromes represent a vast, largely heterogeneous group of disorders characterized by neurological and dermatological manifestations, reflecting the common embryonic origin of epidermal and neural tissues. In the present report, we describe a novel neurocutaneous syndrome characterized by cerebral dysgenesis, neuropathy, ichthyosis, and keratoderma (CEDNIK syndrome). Using homozygosity mapping in two large families, we localized the disease gene to 22q11.2 and identified, in all patients, a 1-bp deletion in *SNAP29,* which codes for a SNARE protein involved in vesicle fusion. SNAP29 expression was decreased in the skin of the patients, resulting in abnormal maturation of lamellar granules and, as a consequence, in mislocation of epidermal lipids and proteases. These data underscore the importance of vesicle trafficking regulatory mechanisms for proper neuroectodermal differentiation.

Introduction

Endocytosis and exocytosis, which are a hallmark of eukaryotic cells, involve tightly orchestrated mechanisms ensuring trafficking of numerous molecules and particles through the formation of membrane carriers, often vesicles (Deitcher 2002). Membrane fusion between vesicles and target membranes, a critical step in these processes, is mediated by a large number of the so-called soluble n-ethylmaleimide sensitive factor attachment protein (SNAP) receptor (SNARE) proteins (Bonifacino and Glick 2004). Two classes of SNAREs can be distinguished: v-SNAREs, located on vesicular membranes, and t-SNAREs, located on target membranes. SNAREs self-assemble into extremely stable four-helix bundles, composed of two cognate parts, which mediate fusion between vesicle and target membrane (Ungar and Hughson 2003). SNAP proteins are ubiquitous t-SNARE proteins that have been shown to promote membrane fusion in numerous physiological systems (Ungar and Hughson 2003).

To date, very few genetic diseases associated with mutations in genes coding for modulators of vesicle trafficking have been described (Chediak Higashi syndrome [MIM 214500]; Griscelli syndrome [MIM 214450, MIM 607624]; Hermansky-Pudlak syndrome [MIM 203300]; chylomicron retention disease [MIM 246700]; familial hemophagocytic lymphohistiocytosis type 4 [MIM 267700]) (Barbosa et al. 1996; Pastural et al. 1997; Menasche et al. 2000; Huizing and Gahl 2002; Jones et al. 2003; Gissen et al. 2004; zur Stadt et al. 2005), and none caused by mutations in genes coding for SNAP molecules have been reported, possibly owing to a large degree of functional redundancy among SNARE proteins or to early lethality associated with mutations in these genes. The present report describes the severe clinical consequences of abnormal expression of a SNAP protein in humans.

Material and Methods

Patients and Biological Materials

All participants or their legal guardians provided written and informed consent according to a protocol ap-

Received April 22, 2005; accepted for publication June 6, 2005; electronically published June 20, 2005.

Address for correspondence and reprints: Dr. Eli Sprecher, Laboratory of Molecular Dermatology, Department of Dermatology, Rambam Medical Center, Haifa, Israel. E-mail: e_sprecher@rambam.health.gov.il

0002-9297/2005/7702-0007$15.00

Table 1

***SNAP29* Oligonucleotide Sequences**

Process and Exon	Oligonucleotide Sequence		Annealing Temperature (°C)
	Forward	Reverse	
Genomic DNA amplification:			
1	F-GGAGTTCGCGCGACGACCGC	R-CAAGAATCTATGCTAGGCAAC	60
2	F-GATGACAGTACCCGTCTCCAG	R-GCACTGACGTGGACTGAAAGTC	60
3	F-GAGTTTGGCACAGAGGAGGC	R-CTTTGGCTAGCATGGGTGATGC	60
4	F-CATGAGCCTGCGCTGTGCTC	R-GACAGTGGCTTACAGAAGCTG	60
5	F-GACAGTGGCTTACAGAAGCTG	R-CATCACAATAGAGTGGAAATC	60
dHPLC screening:			
1	F-GCGGACAGGCAGCAGTACTTG	R-CAAGAATCTATGCTAGGCAAC	60
RT-PCR:			
1–5	F-GAGTCCTGGAGCGCACAGAGAAGATG	R-CAGCTCATCTAGGTTGCTGTCGATC	60
Quantitative real-time PCR:			
3–4	F-GAAGCTATAAGTACAAGTAAAG	R-CATCAGTACTCATGGCAGAAC	55

proved by the local Helsinki Committee and by the Committee for Genetic Studies of the Israeli Ministry of Health. Blood samples were drawn from all family members, and DNA was extracted according to standard procedures. Skin-biopsy samples were fixed either in formaldehyde for subsequent immunohistochemistry, in Karnowski's fixative for transmission electron microscopy, or in paraformaldehyde for immunoelectron microscopy. Fibroblast cell cultures were obtained from punch biopsies from patients or healthy controls after written informed consent was obtained, and they were maintained in DMEM supplemented with fetal calf serum 10%.

Transformation of Fibroblasts by SV40 Large T-Antigen Transfection

Fibroblasts, grown in 10-cm plates, were stably transfected with 10 μg of a plasmid containing the SV40 large T-antigen coupled to the SV40 early promoter (a gift from Dr. Danny Canaani, Tel Aviv University, Israel) (Canaani et al. 1986), by use of 20 μl Lipofectamine 2000 transfection reagent (Invitrogen), according to the manufacturer's instructions. Twelve days later, all colonies in each plate were trypsinized and split. Transformation was confirmed by indirect immunofluorescence. Cells, grown on cover slips, were fixed with 4% paraformaldehyde and were incubated first with a monoclonal anti-SV40 large T-antigen antibody (Gurney et al. 1980) and then with Cy3-conjugated goat anti-mouse secondary antibodies (Jackson Immunoresearch Laboratories).

Genotyping

Genomic DNA was PCR amplified using either fluorescently labeled primer pairs (PE Applied Biosystems) or, for fine mapping, nonlabeled primer pairs. PCR conditions were: 95°C for 4 min, followed by 35 cycles of 95°C for 30 s, 55°C for 30 s, and 72°C for 30 s, with a final extension step of 72°C for 5 min. For semiautomated genotyping, PCR products were separated by PAGE on an ABI 310 sequencer system, and allele sizes were determined with Genescan 3.1 and Genotyper 2.0 software. For manual genotyping, amplicons were electrophoresed on 6% acrylamide gels, followed by silver staining. Multipoint LOD score analysis was performed with the SuperLink software (Fishelson and Geiger 2002), under the assumptions of autosomal recessive inheritance and a mutation frequency of 0.001. Allele frequencies were calculated from analysis of a pool of population-matched DNA samples.

Sequencing

Genomic DNA was PCR amplified using primer pairs encompassing all exons and exon-intron boundaries of the *SNAP29* gene (MIM 604202) (table 1). Gel-purified (QIAquick gel extraction kit, Qiagen) amplicons were subjected to bidirectional DNA sequencing using the BigDye terminator system on an ABI Prism 3100 sequencer (PE Applied Biosystems).

To confirm and screen for the 220delG mutation, we used WAVE analysis (Transgenomic). PCR products were denatured at 95°C for 5 min and were cooled to 65°C down a temperature gradient of 1°C/min. Five μl of each sample were applied to a preheated C18 reversed phase column based on nonporous polystyrene-divinyl-benzene particles (DNA-Sep Cartridge, Transgenomic). DNA was eluted within a linear acetonitrile gradient consisting of buffer A (0.1 M triethylammonium acetate (TEAA)/ buffer B (0.1 M TEAA, 25% acetonitrile) (Transgenomic). The melting profile of the DNA fragment was determined using Wavemaker 4.2 software and the Stanford DHPLC Melt program (Bercovich and Beaudet 2003).

RT-PCR

For semiquantitative RT-PCR, total RNA was extracted from cultured fibroblasts harvested from skin-

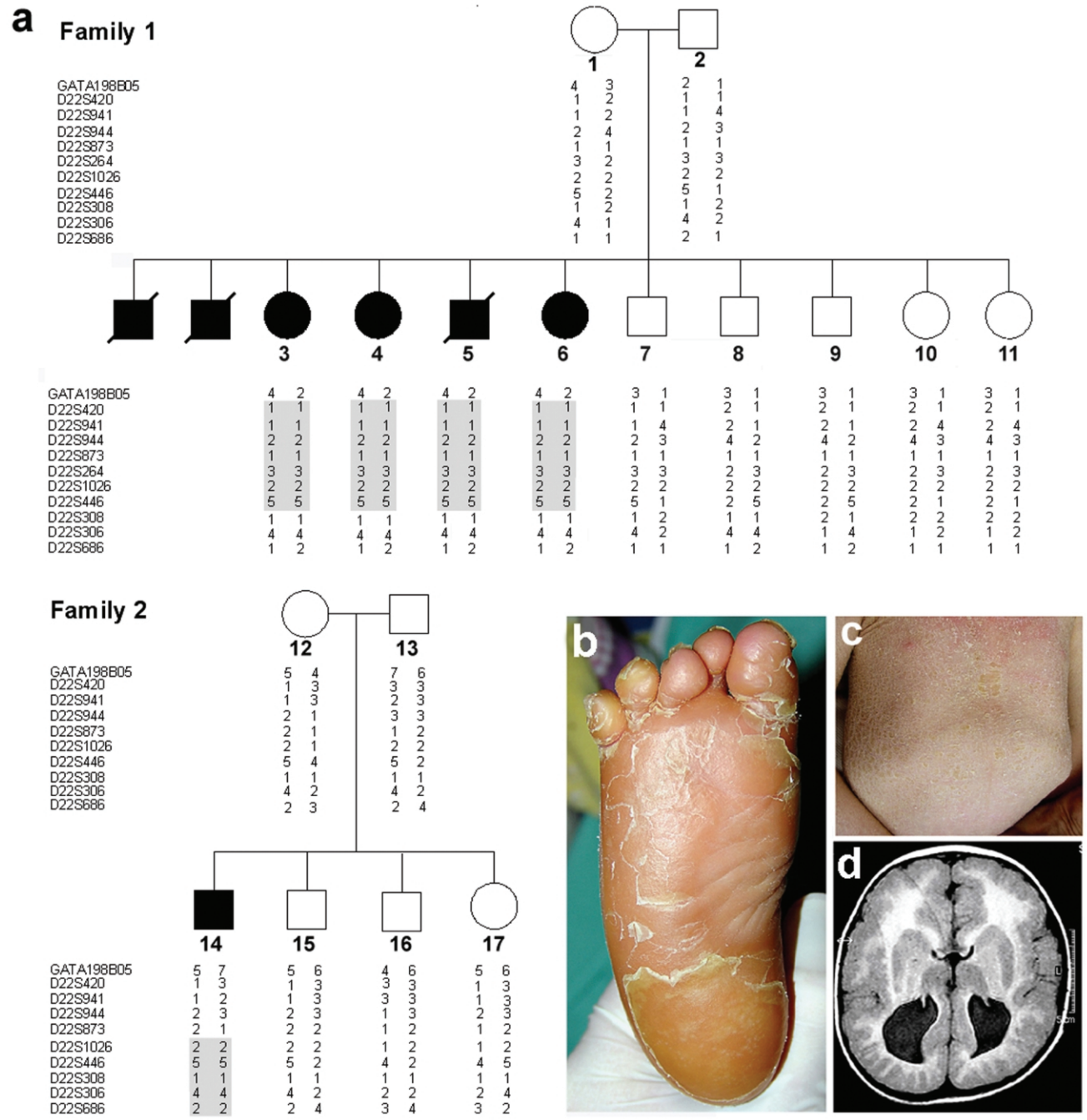

Figure 1 Family trees, genotyping, and clinical spectrum of CEDNIK syndrome. *a,* Haplotype analysis in two families affected with CEDNIK syndrome, performed using polymorphic microsatellite markers on 22q11.2. Homozygous disease-associated haplotypes for each family are marked in gray. *b,* Severe thickening (keratoderma) of the plantar skin in patient 3. *c,* Lamellar ichthyosis over the abdominal surface in patient 14. *d,* Axial T1 (SE) weighted MR image demonstrating cortical dysplasia and pachygyria with polymicrogyria, as well as typical absence of corpus callosum, in patient 5.

biopsy samples (RNeasy extraction kit, Qiagen) and was amplified using the TITAN One Tube RT-PCR kit (Roche Molecular Biochemicals) and intron-crossing primer pairs specific for *SNAP29* (table 1) or *ACTB* (MIM 102630), encoding β-actin (forward, F-CCAAGGCCAACCGCG-AGAAGATGAC; reverse, R-AGGGTACATGGTGGT-GCCGCCAGAC). PCR conditions were: 50°C for 30 min; 94°C for 2 min; 10 cycles of 94°C for 30 s, 60°C

for 30 s, and 68°C for 90 s; 25 cycles of 94°C for 30 s, 60°C for 30 s, and 68°C for 90 s + 5 additional s at each cycle; and a final extension step at 68°C for 7 min.

For quantitative real-time PCR, cDNA was synthesized from 1 μg of total RNA extracted from cultured fibroblasts using the Reverse-iT first strand synthesis kit (ABgene) and random hexamers. cDNA PCR amplification was performed using the Absolute QPCR SYBR Green Mix (ABgene) on a Rotor-Gene 3000 multifilter system (Corbett Research) with primer pairs specific for *SNAP29* (table 1) or *ACTB* (F-TTGCCGACAGGATGCAGAAGGA and R-AGGTGGACAGCGAGGCCAGGAT). To ensure the specificity of the reaction conditions, at the end of the individual runs, the melting temperature (T_m) of the amplified products was measured to confirm its homogeneity. Cycling conditions were as follows: 95°C for 15 min; 95°C for 1 s, 55°C for 5 s, and 72°C for 5 s for a total of 40 cycles. Each sample was analyzed in triplicate. For quantification, standard curves were obtained using serially diluted cDNA amplified in the same real-time PCR run. Results were normalized to β-actin mRNA levels. After the quantification procedure, the products were resolved by 2.5% agarose gel electrophoresis to confirm that the reaction had amplified the correct DNA fragments of known size.

Western Blotting

Cells were homogenized in lysis buffer (10 mM Hepes, 100 mM NaCl, 1 mM $MgCl_2$, 0.5% NP-40, and a protease-inhibitors mix including 1 mM PMSF and 1 μg/ml aprotinin and leupeptin [Sigma]). After centrifugation at 10,000 g for 15 min at 4°C, proteins were electrophoresed through a 10% SDS-PAGE and transferred onto a nitrocellulose membrane (Schleicher Schuell). After 1 h blocking with PBS containing 5% skim milk, blots were interacted with rabbit anti-SNAP29 antibodies (Rotem-Yehudar et al. 2001). The blots were washed three times with TBS-Tween (20 mM Tris HCl, 4 mM Tris base, 140 mM NaCl, 1 mM EDTA, 0.1% Tween-20). After incubation with secondary HRP-conjugated goat anti-rabbit IgG antibodies (Jackson ImmunoResearch) and subsequent washings, proteins were detected using the western blotting Luminol Reagent (Santa Cruz Biotechnology). To compare the amount of protein in the different samples, the blots were reprobed with anti-Erk antibodies (Santa Cruz Biotechnology).

Immunohistochemistry

Formaldehyde-fixed 5-μm paraffin-embedded sections were treated with 3% H_2O_2 in methanol for 15 min at room temperature, were warmed in a microwave oven in citrate buffer for 15 min at 90°C, and were stained with polyclonal anti-SNAP29 antibodies (Abnova Corporation), anti-keratin 14 antibodies (BioGenex), or preimmune rabbit antiserum for 1 h at room temperature. After extensive washings in phosphate-buffered saline, the antibodies were revealed using the ABC technique (Zymed), and the slides were counterstained using hematoxylin.

Electron Microscopy

Transmission electron microscopy (TEM) and immunoelectron microscopy (IEM) analyses were performed as described elsewhere (Ishida-Yamamoto et al. 2005). For IEM, ultrathin cryosections were incubated with antibodies against glucosylceramides (Glycobiotech), kalikrein 5 (KLK5) (Santa Cruz Biotechnology), and KLK7 (Tanimoto et al. 1999).

Results

Clinical Features of CEDNIK Syndrome

We identified two unrelated, consanguineous Arab Muslim families from northern Israel (fig. 1*a*), comprising seven affected individuals (four boys and three girls) displaying a unique constellation of clinical signs. All patients were born at term after an uneventful gestation, with normal APGAR scores and birth weight. Roving eye movements, poor head and trunk control, and failure to thrive were the presenting symptoms during the first 4 mo of life. All patients had progressive microcephaly and facial dysmorphism including elongated faces, antimongolian eye slant, slight hypertelorism, and flat broad nasal root. Palmoplantar keratoderma (fig. 1*b*) and ichthyosis (fig. 1*c*) appeared between 5 and 11 mo of age, with progressive worsening during the 2nd year of life. By the age of 8–15 mo, psychomotor retardation became apparent as major developmental milestones, like unaided sitting and walking, were not attained. Tendon reflexes could not be elicited, and peripheral nerve conduction studies performed in three patients demonstrated low-amplitude responses. Muscle biopsies performed in two patients disclosed neurogenic atrophy and normal activity of the mitochondrial respiratory chain complexes. Ophthalmologic evaluation revealed hypoplastic optic disk; electrophysiological studies were suggestive of reduced conductance from peripheral retina and macular atrophy. Mild sensorineural deafness was demonstrated in three patients studied. Brain MRI performed on four patients showed various degrees of corpus callosum abnormalities and cortical dysplasia, with pachygyria and polimicrogyria (fig. 1*d*). Three male patients died of aspiration pneumonia between 5 and 12 years of age. To date, four patients, aged 5–13 years, are alive, with features including severe psychomotor retardation, ichthyosis, and palmoplantar keratoderma.

The results of routine laboratory studies, plasma and urinary amino acids, urinary organic acids, serum lac-

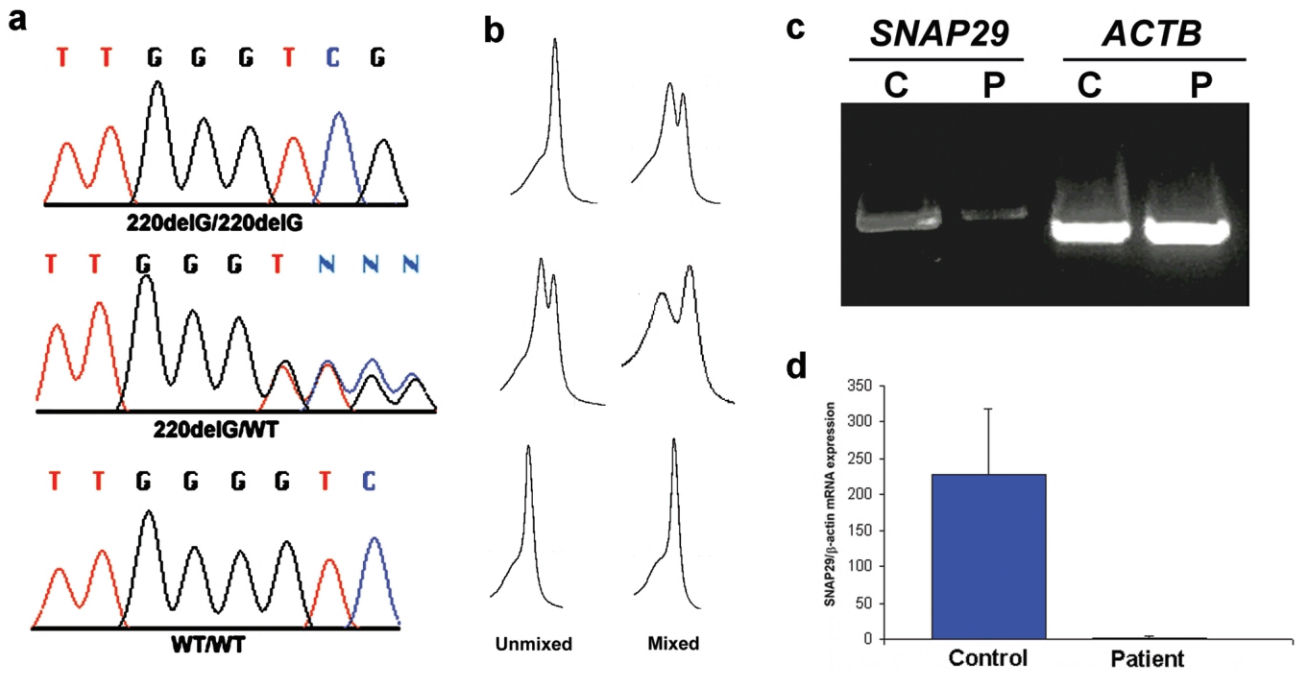

Figure 2 Mutation analysis and gene expression. *a,* Sequence analysis revealed a homozygous G deletion at *SNAP29* cDNA position 220 in all affected individuals of both families (*upper panel*). All obligatory carriers were shown to carry the mutation in a heterozygous state (*middle panel*). The wild-type sequence is given for comparison (*lower panel*). *b,* The corresponding dHPLC tracings obtained by running PCR samples unmixed and mixed with control DNA are depicted. *c,* Expression of *SNAP29* and *ACTB,* coding for β-actin, assessed using RT-PCR in fibroblasts harvested from a patient (P) and from a healthy control individual (C). Note the lower amounts of the *SNAP29* RT-PCR products in the patient relative to the control. *d,* Quantitative real-time PCR analysis for gene expression of *SNAP29* in fibroblasts obtained from control and patient skin. Expression levels are expressed as absolute values normalized relative to β-actin RNA levels.

tate, copper, and ceruloplasmin were within normal limits. Karyotype was normal. Using a battery of enzymatic and biochemical assays, as well as lipid staining in leukocytes and hair microscopy, we excluded a large number of syndromes with closely related clinical manifestations, including Sjogren Larsson syndrome (MIM 270200), peroxisomal disorders, congenital disorders of N- and O-glycosylation, Chanarin-Dorfman disease (MIM 275630), trichothiodystrophy (MIM 601675), Gaucher disease (MIM 230900), steroid sulfatase (MIM 308100), and multiple sulfatase deficiency (MIM 272200).

Mapping of CEDNIK Syndrome

Given the apparent rarity of the syndrome and the fact that the two affected families were consanguineous and lived a few miles from one another, we assumed the existence of a single homozygous causative mutation. We therefore established the genotypes at 332 microsatellite loci of five patients from whom DNA was available and scrutinized our results for regions of homozygosity. A homozygous haplotype spanning 4 Mb on 22q11.2 was found to be shared by all affected individuals and to be absent or carried in a heterozygous state by other healthy family members (not shown). We subsequently genotyped all family members, using 13 markers saturating the putative disease interval. Multipoint LOD score analysis generated a maximum score of 4.85 at marker *D22S446*. Haplotype analysis identified a critical recombination event in individual 8 and loss of homozygosity in individual 14, at markers *D22S308* and *D22S873,* respectively, thereby establishing the telomeric and centromeric boundaries of the disease-associated interval.

SNAP29 Mutation Analysis

The CEDNIK-associated interval, spanning ~2 Mb, was found to harbor 84 genes, among which *SNAP29,* coding for a SNARE protein involved in intracellular vesicle fusion, was chosen as our prime candidate because it modulates critical physiological processes in the central and peripheral nervous system (Su et al. 2001). Sequencing of this gene revealed in all patients a G deletion at cDNA position 220 (starting from ATG) (fig. 2*a*), which was predicted to result in frameshift and in the synthesis of a significantly truncated protein due to premature termination of translation 28 amino acids

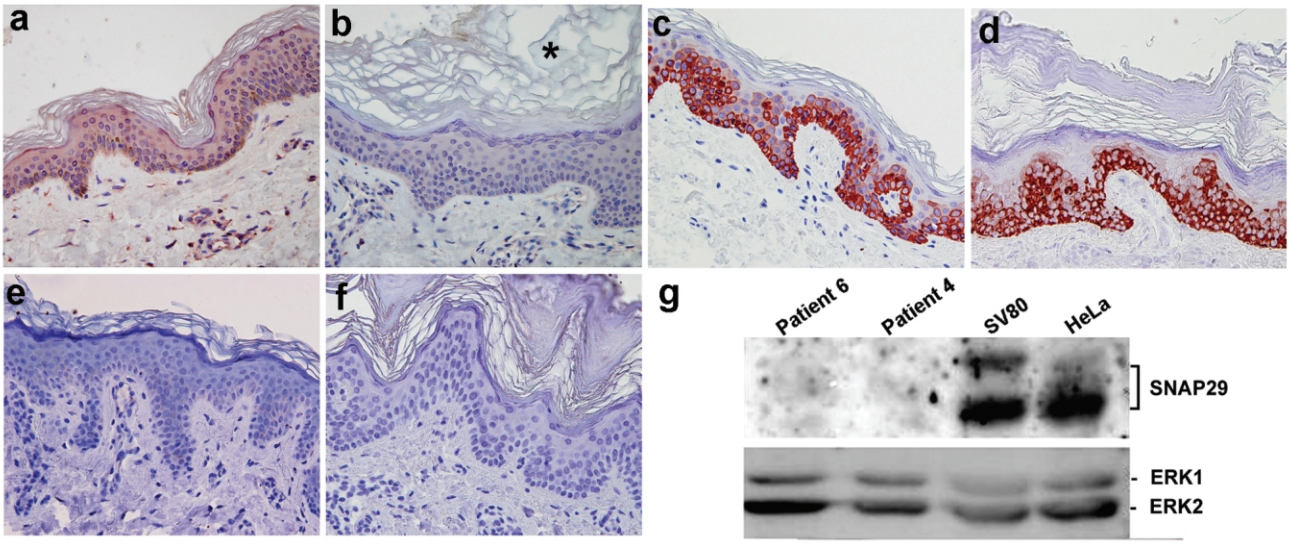

Figure 3 SNAP29 protein expression. Skin biopsy sections obtained from a control individual (*a, c,* and e) and a patient with CEDNIK (*b, d,* and *f*) were stained with antibodies directed against SNAP29 (*a* and *b*) and keratin 14 (*c* and *d*) and with preimmune rabbit antiserum (*e* and *f*). Note the very thickened stratum corneum (hyperkeratosis), marked by an asterisk (*). Cytoplasmic staining for SNAP29 shows positive results in keratinocytes as well as dermal fibroblasts in control skin, but not in the skin of the patient (original magnification × 400). *g,* To confirm the immunostaining results, protein was extracted from transformed fibroblast cell cultures established from patient skin (patients 4 and 6), from control transformed skin fibroblasts (SV80), and from HeLa cells. Cell lysates containing 80 μg of protein were electrophoresed through 10% SDS-PAGE, and the corresponding immunoblot was reacted with anti-SNAP29 antibodies. Detection was performed with HRP-conjugated goat anti-rabbit antibodies. Membranes were reblotted with anti-Erk antibodies to control for protein loading.

downstream of the mutation. Using dHPLC heteroduplex analysis, we confirmed segregation of the mutation in the two families (fig. 2*b*) and excluded the mutation from a panel of 200 population-matched control chromosomes.

SNAP29 Expression in Skin of Patients with CEDNIK Syndrome

The 220delG mutation in SNAP29 gene was found to be associated with decreased levels of *SNAP29* transcripts (fig. 2*c*), possibly reflecting nonsense-mediated mRNA decay. Using quantitative RT-PCR, we found that *SNAP29* RNA expression was decreased 99-fold in patient fibroblasts relative to control fibroblasts (fig. 2*d*). To assess the consequences of the mutation at the protein level, we stained skin-biopsy samples obtained from patients and control individuals with anti-recombinant SNAP29 antiserum. *SNAP29* was found to be expressed by virtually all cells in the normal epidermis and dermis (fig. 3*a*). In contrast, SNAP29 expression was markedly reduced in the skin of affected individuals (fig. 3*b*). This decrease in SNAP29 expression was specific, since the expression of unrelated proteins such as keratin 14 was unchanged (fig. 3*c* and 3*d*) and staining with preimmune rabbit serum showed negative results (fig. 3*e* and 3*f*). We then confirmed these results using western blot analysis of protein extracted from SV40-transformed normal fibroblasts and SV40-transformed fibroblasts grown from skin-biopsy samples obtained from two patients (fig. 3*g*). Similar results were obtained using primary fibroblast cell cultures (not shown). Thus, 220delG mutation results in SNAP29 deficiency in the skin of patients with CEDNIK syndrome.

Ultrastructural Consequences of SNAP29 Deficiency in CEDNIK Syndrome

Lamellar granules are abundant organelles typically found in the upper epidermal layers and responsible for delivering to the stratum corneum lipids, proteases, and their inhibitors during the process of epidermal barrier formation (Fartasch 2004). A large body of evidence supports the concept that lamellar granules originate from the Golgi complex (Ishida-Yamamoto et al. 2005). In parallel, a number of studies have shown that SNAP29, in contrast with other SNAP proteins (Gonelle-Gispert et al. 2000; Feng et al. 2002), is prominently found in intracellular membrane structures (Steegmaier et al. 1998; Ugur and Jones 2000; Hohenstein et al. 2001) and have suggested a specific role for SNAP29 in mediating Golgi trafficking (Wong et al. 1999). To assess the possibility that SNAP29 deficiency interferes with epidermal granule maturation, we examined skin-biopsy samples obtained from a CEDNIK patient by TEM. The most striking ultrastructural abnormality in the patient epidermis

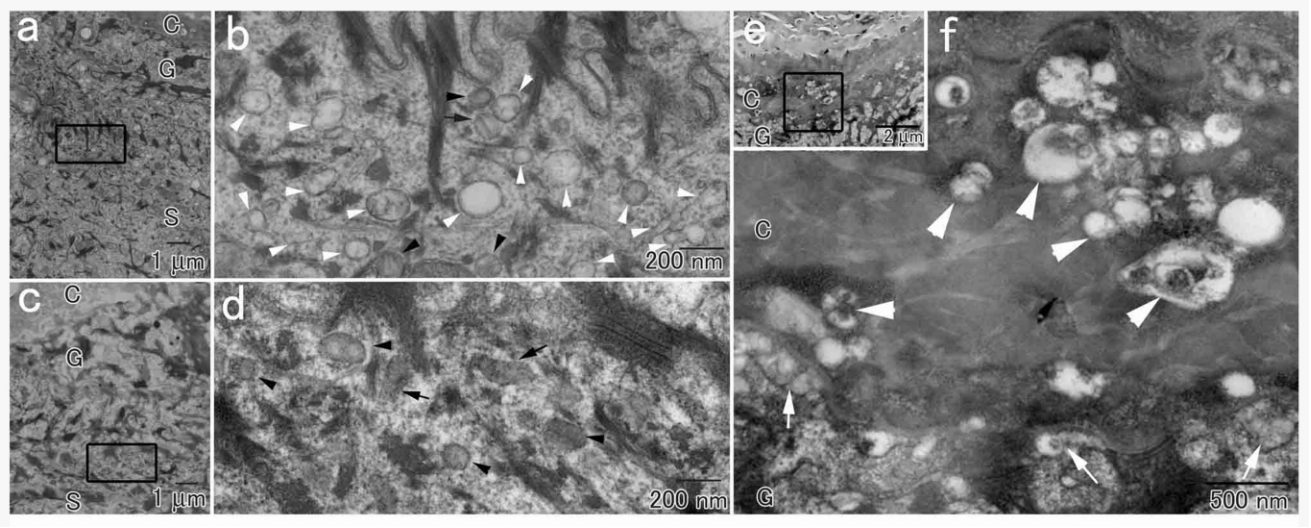

Figure 4 Transmission electron micrograph of a skin-biopsy sample obtained from a patient (*a, b, e,* and *f*) and from a healthy control individual (*c* and *d*). Panels b, d, and f show higher-magnification views of the areas marked in panels a, c, and e, respectively. In addition to normal appearing lamellar granules with (*black arrows*) or without (*black arrowheads*) lamellar internal structures, numerous empty vesicles (*white arrowheads*) are seen in the patient epidermis (*b*) but not in the control skin (*d*). *e* and *f,* The extracellular spaces between the most superficial granular cells and the cornified cells in the patient skin contain secreted lamellar granule contents (*white arrows* in panel *f*). In addition, countless abnormal vesicles are observed in the lower stratum corneum (*white arrowheads*). The letters C, G, and S identify the epidermal cornified, granular, and spinous cell layers, respectively.

was the presence of countless clear vesicles in the spinous and granular epidermal layers (fig. 4*a* and 4*b*) that were not found in control epidermis (fig. 4*c* and 4*d*). Vesicles of various sizes and contents were also present, abnormally, in the lower layers of the significantly thickened stratum corneum in patient skin (fig. 4*e* and 4*f*) but not in normal skin (not shown). It is of note that normal-looking lamellar granules, loaded with lipid molecules, were also seen (fig. 4*b*), and they were released into the extracellular space between the superficial granular and cornified layers (fig. 4*e* and 4*f*). We did not observe any additional abnormality in other epidermal structures.

Epidermal differentiation is critically dependent on proper spatial deposition of lipids and proteolytic enzymes, which contribute to the formation of the skin barrier and mediate desquamation, respectively (Ishida-Yamamoto et al. 2005). Because the transfer of these molecules to the stratum corneum is, in turn, dependent on correct formation of lamellar granules, and because lamellar granule maturation was found to be abnormal in CEDNIK syndrome (fig. 4), we assessed the distribution of glucosylceramides in patient skin, using IEM. Glucosylceramides are precursor molecules for ceramides, the most abundant intracorneal lipids, and are normally secreted between granular and cornified epidermal cells (Ishida-Yamamoto et al. 2005) (fig. 5, *left panel*). In the skin of our patients, considerable amounts of glucosylceramides were retained, abnormally, within the cells of lower stratum corneum (fig. 5, *middle panel*) and numerous vesicles with positive glucosylceramide labeling were seen in the lower cornified layer (fig. 5, *right panel*), indicating that lamellar granules are not correctly secreted in the skin of patients with CEDNIK syndrome. Abnormal vesicles in the cornified cells were also found to contain KLK5 and KLK7, two proteases of major importance for normal desquamation (Caubet et al. 2004) (not shown).

Discussion

In the present study, we describe a novel neurocutaneous disease, termed "CEDNIK syndrome," characterized by severe developmental abnormalities of the nervous system as well as aberrant differentiation of the epidermis. We show that this disorder results from decreased expression of SNAP29, a SNARE protein involved in vesicle fusion. Although neural tissues were not available for examination, ultrastructural features of the syndrome in the skin of patients, including the presence of abnormal vesicles in the granular and lower cornified cell layers of the epidermis, are consonant with deranged function of SNARE-mediated vesicle transport/fusion. Interestingly, abnormal vesicles were also observed in dermal fibroblasts (not shown), suggesting a generalized defect in vesicle trafficking in patient tissues. Although, to our knowledge, similar ultrastructural features have

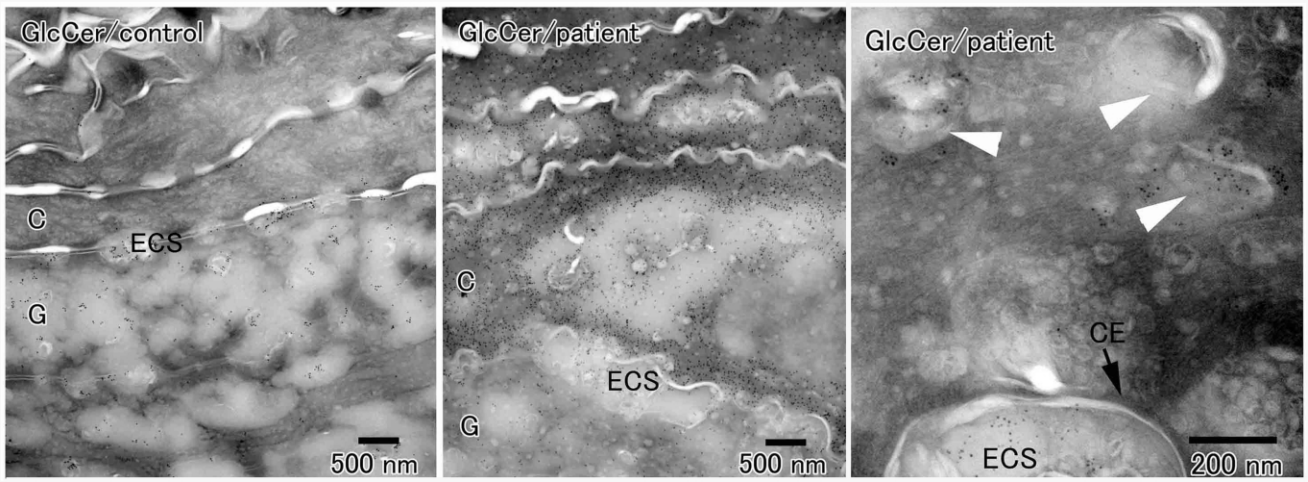

Figure 5 Immunoelectron microscopy of skin-biopsy samples obtained from two CEDNIK patients and a control individual with antibodies directed against glucosylceramides (GlcCer). Glucosylceramides appear as black dots. In the control samples, glucosylceramides are found in lamellar granules, and they are secreted between the epidermal granular cells (G) and cornified cells (C) (*left panel*). By contrast, in patient skin, only a small proportion of glucosylceramide-positive granules is secreted into the extracellular spaces (ECS) between the granular and cornified cells, a large amount of glucosylceramides is found in the lower cornified cells (*middle panel*), which are shown to retain a very large number of glucosylceramide-positive vesicles (*white arrowheads* in *right panel*). The black arrow marks the cornified cell envelope (CE).

never previously been described in a human disease, they bear striking resemblance to the phenotype observed in mutant yeasts with abnormal SNARE complex function causing defective fusion of transport vesicles with the Golgi apparatus (Bonifacino and Glick 2004). As mentioned above, SNAP29 has been shown to play an important role in Golgi trafficking (Wong et al. 1999).

Abnormal SNAP29-mediated vesicle fusion may explain the major clinical features characteristic of CEDNIK syndrome. Indeed, numerous studies have underscored the importance of the SNARE machinery during brain development, axonal growth, synaptogenesis, and neurotransmission (Hepp and Langley 2001; Chen and Olson 2005). SNARE proteins have also been shown to play an important role in the development of the retina (West-Greenlee et al. 1998). The prominent ophthalmologic signs observed in patients with CEDNIK syndrome—including roving eye movements during the first months of life (or even at birth, in one patient), early macular atrophy, and reduced conductance from peripheral retina demonstrated by electrophysiological studies—together suggest a pivotal function for SNAP29 in the development of the visual system. SNAP29 regulates neurotransmitter release by slowing the recycling of the fusion machinery and down-regulating synaptic vesicle turnover (Su et al. 2001; Pan et al., in press). The process of synaptic vesicle recycling, including SNARE complex formation and dissociation, is essential for ongoing synaptic transmission (Sudhof 2004). SNAP29 deficiency may therefore explain the development of the severe neuropathy displayed by patients with CEDNIK syndrome. Moreover, the skin findings in CEDNIK syndrome are likely to result from abnormal lamellar granule maturation and secretion (figs. 4 and 5). Although in normal skin, lamellar granules release lipids and proteases beneath the stratum corneum, reinforcing the epidermal barrier and mediating desmosome dissolution during desquamation, respectively, in CEDNIK syndrome, glucosylceramide and kallikrein-containing granules are aberrantly retained in the stratum corneum, leading to abnormal barrier formation and retention hyperkeratosis (fig. 6).

CEDNIK syndrome includes a number of features overlapping with clinical characteristics of other genetic diseases, which is suggestive of intersecting pathophysiologies. For example, lamellar body degeneration has been observed in type II pneumocytes in Hermansky-Pudlak syndrome, another autosomal recessive disorder associated with impaired vesicle trafficking (Nakatani et al. 2000). Also, the occurrence of neurocutaneous signs associated with abnormal distribution of glucosylceramides in the skin of patients with CEDNIK syndrome is reminiscent of the clinical phenotype resulting from decreased hydrolysis of glucosylceramide to ceramide in type II Gaucher disease (Holleran et al. 1994), where severe ichthyosis can be observed along with neurological deficits.

In conclusion, we have described a novel human genetic disease, caused by decreased expression of SNAP29 and resulting in abnormal vesicle maturation and se-

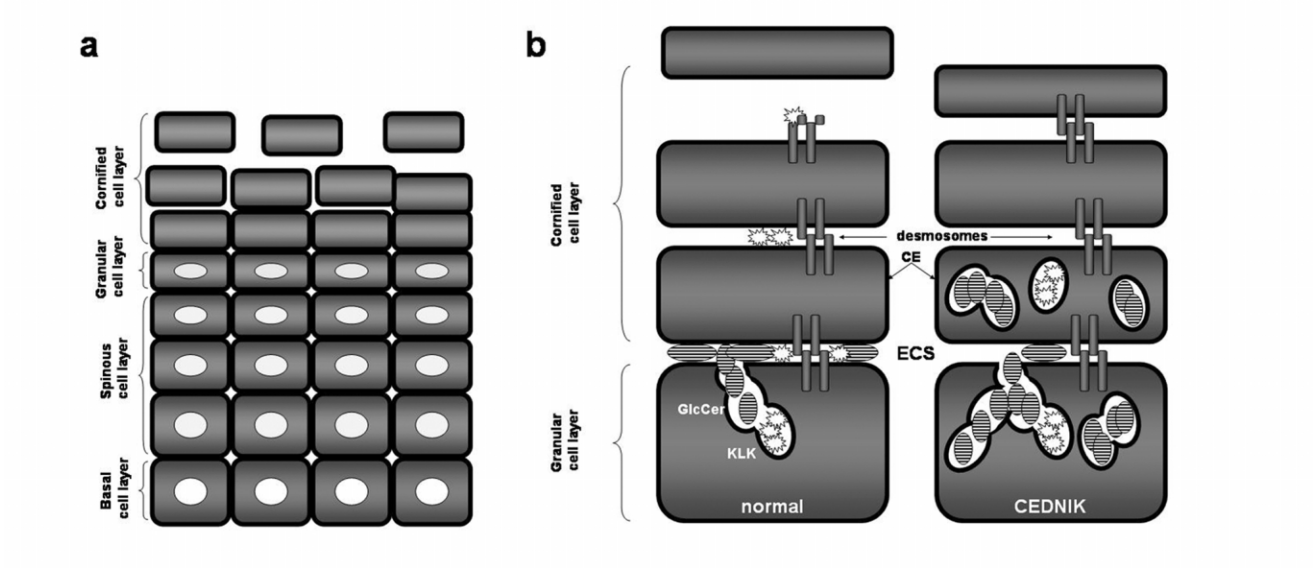

Figure 6 Pathogenesis of CEDNIK syndrome. *a,* Formation of the epidermal barrier occurs at the end of a complex differentiation process during which keratinocytes, derived from the proliferating basal cell layer, sequentially transform into spinous cells, granular cells, and cornified cells as they migrate outwards throughout the epidermis. *b,* The epidermal barrier is composed of the cornified cell envelope (CE), a protein scaffold, which replaces the plasma membrane; intracellular cross-linked and polymerized keratin filament bundles; and extracellular lipid layers. Lipids, such as glucosylceramides (GlcCer), are normally secreted from lamellar granules present in granular cells into the extracellular space (ECS) between the granular and the cornified cell layers. Lamellar granules also secrete proteases, such as KLK5 and KLK7, which dissolve desmosomal plates in the upper cornified cell layers, thereby enabling cells to separate one from the other, a process known as "desquamation." In CEDNIK syndrome, lamellar granules are retained within the cornified cell layer, and the diminished secretion of lipids and proteases in the ECS, causes impaired barrier formation and decreased desquamation, respectively, which explains the increased thickness of the outer epidermal layers in patients.

cretion. These data underscore the importance of the SNARE complex in general and of SNAP29 in particular for normal neuroectodermal differentiation.

Acknowledgments

We are grateful to the family members for their participation in our study. We thank Dr. Vered Friedman, for services in nucleic acid analysis; Ma'ayan Fishelson and Anna Tzemach, for computer assistance; and Dr. Peter Itin, Dr. Gabriele Richard, Dr. Eddie Karnieli, Dr. Tsipora Kra-Oz, Alon Hirshberg, and Dr. Gila Maor, for stimulating discussions. This study was supported in part by grants provided by the Ruth and Allen Ziegler Fund for Pediatric Research (to E.S.) and the Japanese Ministry of Education, Culture, Sports, Science and Technology (to A.I.Y.). Electron microscopy samples were observed at the Electron Microscopy Unit, Central Laboratory for Research and Education, Asahikawa Medical College.

Web Resources

The URLs for data presented herein are as follows:

DHPLC Melt program, http://insertion.stanford.edu/meltdoc.html
Online Mendelian Inheritance in Man (OMIM), http://www.ncbi.nlm.nih.gov/Omim/
Superlink, http://bioinfo.cs.technion.ac.il/pedtool/

References

Barbosa MDFS, Nguyen QA, Tchernev VT, Ashley JA, Detter JC, Blaydes SM, Brandt SJ, Chotai D, Hodgman C, Solari RCE, Lovett M, Kingsmore SF (1996) Identification of the homologous beige and Chediak-Higashi syndrome genes. Nature 382:262–265

Bercovich D, Beaudet AL (2003) Denaturing high-performance liquid chromatography for the detection of mutations and polymorphisms in UBE3A. Genet Test 7:189–194

Bonifacino JS, Glick BS (2004) The mechanisms of vesicle budding and fusion. Cell 116:153–166

Canaani D, Naiman T, Teitz T, Berg P (1986) Immortalization of xeroderma pigmentosum cells by simian virus 40 DNA having a defective origin of DNA replication. Somat Cell Mol Genet 12:13–20

Caubet C, Jonca N, Brattsand M, Guerrin M, Bernard D, Schmidt R, Egelrud T, Simon M, Serre G (2004) Degradation of corneodesmosome proteins by two serine proteases of the kallikrein family, SCTE/KLK5/hK5 and SCCE/KLK7/hK7. J Invest Dermatol 122:1235–1244

Chen EH, Olson EN (2005) Unveiling the mechanisms of cell-cell fusion. Science 308:369–373

Deitcher D (2002) Exocytosis, endocytosis, and development. Semin Cell Dev Biol 13:71–76

Fartasch M (2004) The epidermal lamellar body: a fascinating secretory organelle. J Invest Dermatol 122:XI–XII

Feng D, Crane K, Rozenvayn N, Dvorak AM, Flaumenhaft R (2002) Subcellular distribution of 3 functional platelet SNARE proteins: human cellubrevin, SNAP-23, and syntaxin 2. Blood 99:4006–4014

Fishelson M, Geiger D (2002) Exact genetic linkage computations for general pedigrees. Bioinformatics 18:S189–S198

Gissen P, Johnson CA, Morgan NV, Stapelbroek JM, Forshew T, Cooper WN, McKiernan PJ, Klomp LW, Morris AA, Wraith JE, McClean P, Lynch SA, Thompson RJ, Lo B, Quarrell OW, Di Rocco M, Trembath RC, Mandel H, Wali S, Karet FE, Knisely AS, Houwen RH, Kelly DA, Maher ER (2004) Mutations in VPS33B, encoding a regulator of SNARE-dependent membrane fusion, cause arthrogryposis-renal dysfunction-cholestasis (ARC) syndrome. Nat Genet 36:400–404

Gonelle-Gispert C, Molinete M, Halban PA, Sadoul K (2000) Membrane localization and biological activity of SNAP-25 cysteine mutants in insulin-secreting cells. J Cell Sci 113: 3197–3205

Gurney EG, Harrison RO, Fenno J (1980) Monoclonal antibodies against simian virus 40 T antigens: evidence for distinct sublcasses of large T antigen and for similarities among nonviral T antigens. J Virol 34:752–763

Hepp R, Langley K (2001) SNAREs during development. Cell Tissue Res 305:247–253

Hohenstein AC, Roche PA (2001) SNAP29 is a promiscuous syntaxin-binding SNARE. Biochem Biophys Res Commun 285:167–171

Holleran WM, Ginns EI, Menon GK, Grundmann JU, Fartasch M, McKinney CE, Elias PM, Sidransky E (1994) Consequences of beta-glucocerebrosidase deficiency in epidermis: ultrastructure and permeability barrier alterations in Gaucher disease. J Clin Invest 93:1756–1764

Huizing M, Gahl WA (2002) Disorders of vesicles of lysosomal lineage: the Hermansky-Pudlak syndromes. Curr Mol Med 2:451–467

Ishida-Yamamoto A, Deraison C, Bonnart C, Bitoun E, Robinson R, O'Brien TJ, Wakamatsu K, Ohtsubo S, Takahashi H, Hashimoto Y, Dopping-Hepenstal PJ, McGrath JA, Iizuka H, Richard G, Hovnanian A (2005) LEKTI is localized in lamellar granules, separated from KLK5 and KLK7, and is secreted in the extracellular spaces of the superficial stratum granulosum. J Invest Dermatol 124:360–366

Jones B, Jones EL, Bonney SA, Patel HN, Mensenkamp AR, Eichenbaum-Voline S, Rudling M, Myrdal U, Annesi G, Naik S, Meadows N, Quattrone A, Islam SA, Naoumova RP, Angelin B, Infante R, Levy E, Roy CC, Freemont PS, Scott J, Shoulders CC (2003) Mutations in a Sar1 GTPase of COPII vesicles are associated with lipid absorption disorders. Nat Genet 34:29–31

Menasche G, Pastural E, Feldmann J, Certain S, Ersoy F, Dupuis S, Wulffraat N, Bianchi D, Fischer A, Le Deist F, de Saint Basile G (2000) Mutations in RAB27A cause Griscelli syndrome associated with haemophagocytic syndrome. Nat Genet 25:173–176

Nakatani Y, Nakamura N, Sano J, Inayama Y, Kawano N, Yamanaka S, Miyagi Y, Nagashima Y, Ohbayashi C, Mizushima M, Manabe T, Kuroda M, Yokoi T, Matsubara O (2000) Interstitial pneumonia in Hermansky-Pudlak syndrome: significance of florid foamy swelling/degeneration (giant lamellar body degeneration) of type-2 pneumocytes. Virchows Arch 437:304–313

Pan PY, Cai Q, Lin L, Lu PH, Duan SM, Sheng ZH. SNAP-29–mediated modulation of synaptic transmission in cultured hippocampal neurons. J Biol Chem (in press) (accepted manuscript version available at http://www.jbc.org/cgi/content/abstract/M502356200v1)

Pastural E, Barrat FJ, Dufourcq-Lagelouse R, Certain S, Sanal O, Jabado N, Seger R, Griscelli C, Fischer A, de Saint Basile G (1997) Griscelli disease maps to chromosome 15q21 and is associated with mutations in the myosin-Va gene. Nat Genet 16:289–292

Rotem-Yehudar R, Galperin E, Horowitz M (2001) Association of insulin-like growth factor 1 receptor with EHD1 and SNAP29. J Biol Chem 276:33054–33060

Steegmaier M, Yang B, Yoo JS, Huang B, Shen M, Yu S, Luo Y, Scheller RH (1998) Three novel proteins of the syntaxin/SNAP-25 family. J Biol Chem 273:34171–3419

Su Q, Mochida S, Tian JH, Mehta R, Sheng ZH (2001) SNAP29: a general SNARE protein that inhibits SNARE disassembly and is implicated in synaptic transmission. Proc Natl Acad Sci USA 98:14038–14043

Sudhof TC (2004) The synaptic vesicle cycle. Annu Rev Neurosci 27:509–547

Tanimoto H, Underwood LJ, Shigemasa K, Yan Yan MS, Clarke J, Parmley TH, O'Brien TJ (1999) The stratum corneum chymotryptic enzyme that mediates shedding and desquamation of skin cells is highly overexpressed in ovarian tumor cells. Cancer 86:2074–2082

Ugur O, Jones TL (2000) A proline-rich region and nearby cysteine residues target XLalphas to the Golgi complex region. Mol Biol Cell 11:1421–1432

Ungar D, Hughson FM (2003) SNARE protein structure and function. Annu Rev Cell Dev Biol 19:493–517

West-Greenlee MH, Finley S, Wilson MC, Jacobson CD, Sakaguchi DS (1998) Transient, high levels of SNAP-25 expression in cholinergic amacrine cells during postnatal development of the mammalian retina. J Comp Neurol 394:374–385

Wong SH, Xu Y, Zhang T, Griffiths G, Lowe SL, Subramaniam VN, Seow KT, Hong W (1999) GS32, a novel Golgi SNARE of 32 kDa, interacts preferentially with syntaxin 6. Mol Biol Cell 10:119–134

zur Stadt U, Schmidt S, Kasper B, Beutel K, Diler AS, Henter JI, Kabisch H, Schneppenheim R, Nurnberg P, Janka G, Hennies HC (2005) Linkage of familial hemophagocytic lymphohistiocytosis (FHL) type-4 to chromosome 6q24 and identification of mutations in syntaxin 11. Hum Mol Genet 14:827–834